

Study the Corrosion Inhibition on the Iraqi Fuel Tanks using Cefoperazone Drug

Akram Mohsin kadhim^{1*}, Rana Afif Anaee², Mohammed Jasim M. Hassan¹,
Munaf Adnan Idan Al-lami³

¹Department of Chemistry, College of Science, Mustansiriyah University, 10052 Baghdad, Iraq.

²Department of Materials Engineering, University of Technology, Baghdad, Iraq.

³Department of Chemical and Environmental Process Engineering, Faculty of Chemical Technology and Biotechnology, Budapest University of Technology and Economics, H-1111 Budapest, Hungary.

*Corresponding contact: akrammohsin1982@gmail.com

Article Info

Received
11/03/2023

Revised
06/04/2023

Accepted
27/04/2023

Published
30/09/2023

ABSTRACT

Corrosion is one of the most important problems that face the petroleum industry, both production and refining, and cause damage to petroleum equipment, tanks, and transmission lines, and increasing maintenance costs. In this study, was adding six concentrations of the drug expired Cefoperzone (Exp CEF) (50, 100, 200, 300, 400, and 500 ppm) to a Simulated Oil Well Water (SOWW), the inhibitive role of (Exp CEF) drug was investigated to Reduce the corrosion risk of carbon steel. Four different temperatures were used to conduct electrochemical tests (303, 313, 323 and 333 K) to achieve the study. The study was then supported by an examination of the inhibited surface using field emission scanning electron microscopy with energy dispersive (FESEM) and (AFM). The results indicated occurring the inhibition by an anodic inhibitor that controls the dissolution of iron from steel gave the highest inhibition efficiency (IE%) by adding 500 ppm, while the calculation of polarization resistance (R_p) gave the highest resistance by 400 ppm through adsorption the added drug to show flakes shaped structures with decreasing surface roughness (R_a) from 307.1 to 83.15 nm after inhibition. The calculation of adsorption isotherm confirmed the obeying of Langmuir adsorption isotherm by giving the coefficient of linear regression was about one in the range of $0.999 \geq R^2 \geq 0.995$, with the spontaneous adsorption that estimated from the negative values of ΔG_{ads}^o and variation in the type of adsorption to be physically or chemically according to the added concentration because of the differential sign of ΔH_{ads}^o . The sign of ΔS_{ads}^o was positive that reflecting the increase in randomness at the metal/solution interface.

KEYWORDS: Carbon steel; Drug; Simulated oil well water; Green inhibitor.

الخلاصة

يعتبر التآكل من أهم المشاكل التي تواجه صناعة البترول سواء الإنتاج أو التكرير ، مما يتسبب في تلف المعدات البترولية والخزانات وخطوط النقل ، وزيادة تكاليف الصيانة. لذلك ، هناك حاجة إلى طرق للتحكم في التآكل في هذه الدراسة التجريبية تم اختبار عقار سيفابيرازون المنتهي الصلاحية بستة تراكيز (50 ، 100 ، 200 ، 300 ، 400 ، 500) جزء بالمليون كمادة مثبطة للتآكل عند أربع درجات حرارية (303 ، 313 ، 323 ، 333) كلفن في وسط ملحي محاكي لمياة الابار النفطية باستخدام الكهروضوئية.

وتم دعم هذه الدراسة بأجراء عدة فحوصات قبل وبعد اضافة المثبط (سيفابيرازون منتهي الصلاحية) ، و اشارت النتائج الى حدوث التثبيط على سطح سبيكة الكربون الصلب حيث اعطت اعلى كفاءة تثبيط عند تركيز 500 جزء بالمليون المثبط واعطت اعلى مقاومة استقطاب عند تركيز 400 جزء بالمليون من خلال امتصاص العقار من قبل سطح السبيكة ، مع تناقص خشونة السطح من 307.1 ، إلى 83.15 نانومتر بعد التثبيط . كما كانت قيم الانتروبي موجبة مما يدل على زيادة العشوائية في واجهة المعدن

INTRODUCTION

Low-carbon steel is the kind of alloy that is employed the most (approximately 85%) in the

construction of various oil equipment, but it is subject to corrosion, just as other metals and alloys [1][2]. Metals and alloys make an effort

to revert to disorder, but an external factor, such as inhibitors, can significantly slow down this process. Because of their anti-corrosive qualities, inhibitors have been the most widely used strategy in the industry for protecting numerous metal surfaces against corrosion in recent years [3]. The technique of introducing compounds that greatly slow down and stop the corrosion process in small doses is known as inhibition. Numerous investigations have been conducted to ascertain the effectiveness of inhibition for organic material, particularly heterocyclic derivatives to lessen the corrosion of metals. Recently, many authors have selected triazole derivatives as anti-corrosive materials in different environments due to several reasons such as the possibility of their preparation with good yields from commercial materials also they contain three nitrogen atoms and π -system. These properties are a reason make the triazoles an excellent class of corrosion inhibitors, which were investigated by many authors, for example, Belghiti *et al.* [4] studied the corrosion inhibition performance of a 4-amino-3,5-bis (disubstituted)-1,2,4-triazole derivatives for mild steel in phosphoric acid solution, the results exhibited that these compounds have good inhibition properties.

In the present work, the Cefoperazone drug which has a chemical formula shown in Figure 1 will be used to inhibit carbon steel in a simulated fuel medium with generation H₂S gas at four temperatures by Potentiostat device.

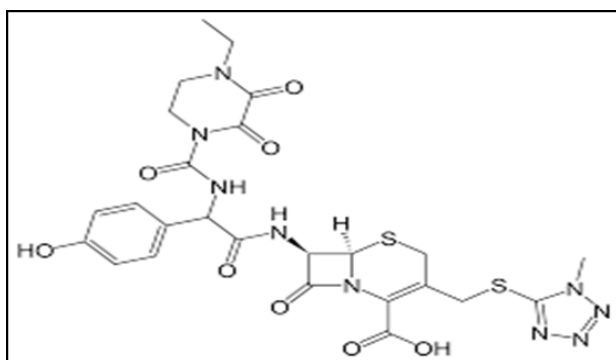


Figure 1: Chemical structure of cefoperazone drug.

MATERIALS AND METHODS

Specimens

Steel samples were brought from the projects department responsible for the design of crude

oil and its derivatives tanks in the Maysan Refinery and the processing complex in the Maysan Oil Company. The obtained results (in wt %) were: C (0.24), Si (0.51), Mn (0.9), P (0.035), S (0.04), Cr (0.0132), Cu (0.2), and Fe (remainder). To achieve the final specimen shape, samples of 2 * 2 cm were prepared in the workshop of the University of Technology. The samples' thickness was decreased by grinding equipment from 6-8 mm to 3-3.2 mm. To create a smooth surface, the samples with a surface area of 2*2 cm² and a thickness of 3 mm were ground and polished with SiC emery sheets (grit 400, 600, 800, 1000, 1200, and 2500). In the final phase, the specimens were cleaned with acetone to remove any remaining grease before being dried and placed in plastic containers for electrochemical analysis.

Corrosive Medium

To simulate the real water of the oil well, 500 ml of water was prepared in the standard measuring flask (SMF) by adding three components (0.305g of anhydrous calcium chloride (CaCl₂), 3.5g of sodium chloride (NaCl) and 0.186g of magnesium chloride (MgCl₂)) to double distilled water (ddH₂O). before conducting the experiment, the smell of hydrogen sulfide (H₂S) gas should be tested by mixing 0.03g of sodium sulfide with concentrated hydrochloric acid (HCL) solution [16].

Characterization Measurements

The polished, inhibited and uninhibited surfaces were imaged using the scanning electron microscopy (SEM) technique, and were measured the elemental components by the energy dispersive X-ray spectroscopy (EDS) test, (TESCAN MIRA3 FRENCH).

In addition, the changes in the surfaces (before and after the inhibition process). Were examined by an atomic-force microscope (AFM; AA3000/220V, Angstrom Advanced, Inc. USA).

Corrosion Test

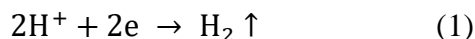
The electrochemical technique used in this study was carried out using a traditional three-electrode system made up of a 1 cm² surface area of a mild steel specimen as a working

electrode and a potentiostat/galvanostat representing the reference electrode. High-purity platinum served as the auxiliary electrode (WINKINK M Lab 200). The overall emulsion solution from simulated oil well water and all the electrochemical experiments (at 303, 313, 323, and 333 K) were performed using a digitally controlled water bath. The working electrode was immersed in the corrosive solution until a steady state was attained between the sample and the electrolyte (with and without the inhibitor). The Curves of Tafel plots were recorded the electrode's current was automatically varied from -15 to +15mA to record the density of corrosion current (i_{corr}), the corrosion potential (E_{corr}), and the Tafel slopes at a scan rate of 1 mA/s (bc and ba).

RESULTS AND DISCUSSION

Electrochemical Properties

Cefoperazone has been added to a simulated fuel medium (SFM) with six concentrations (50, 100, 200, 300, 400, and 500 ppm) to study its role as an inhibitor for carbon steel at four temperatures (303, 313, 323, and 333 K). Figure 2 illustrates the curves of polarization for carbon steel in both the presence and absence of Cefoperazone that shows the cathodic regions where Equ. (1) represents how hydrogen is reduced:



Even in anodic regions, iron atoms dissolve or ionize by the Equ. (2):



The addition of Cefoperazone to the corrosive medium leads to shifting corrosion potential (E_{corr}) toward noble values confirming Equ.(3):

$$C_R \text{ (mm/y)} = 3.27 \times i_corr \text{ (e/\rho)} \quad (3)$$

using the value of equivalent weight (e) and density (ρ) of the substrate. The important parameter uses to estimate the role of inhibition is inhibition that this drug behaves as an anodic inhibitor (i.e., reduces the dissolution of iron

atoms through blocking the anodic sites and then reduces the consumption of the electrons at cathodic sites). After adding Cefoperazone, the density of corrosion current (i_{corr}) reduced, demonstrating the inhibitory effect of this medication, which has a direct relationship to the corrosion rate (C_R), which was computed using the Equ. (4) and is shown in Table 1 [17][18]. In this Table, efficiency (IE%) calculated using the current density values in the absence ($i_{corr,uninhibited \text{ medium}}$) and presence ($i_{corr,inhibited \text{ medium}}$) of the drug as follow [19][20]:

$$IE\% = \left[1 - \frac{i_{corr,inhibited \text{ medium}}}{i_{corr,uninhibited \text{ medium}}} \right] \times 100 \quad (4)$$

The data in Table 1 indicate that the best concentration is 500 ppm which gave the highest IE% values.

To identify the resistance of the metallic material against corrosion, Polarization resistance (R_p) can be utilized by using the Equ. (5):

$$R_p = \left(\frac{\Delta E}{\Delta i} \right)_{\Delta E \rightarrow 0} \quad (5)$$

Where, ΔE is the distinction between the applied potential and the (E_{corr}) and Δi is the polarization current that results.

The Polarization resistance (R_p) can be calculated by the expression [21][22] by Equ.(6):

$$R_p = \frac{b_c \times b_a}{2.303 \times i_{corr}(b_c + b_a)} \quad (6)$$

The data of polarization resistance (R_p) for the drug are shown in Figure 3, which indicates that 400 ppm of Cefoperzone gives the highest resistance for steel surfaces. As shown in Figure 7, the Langmuir and Freundlich isotherms are the most widely employed to describe sorption data from solution Figure 7, Langmuir and Freundlich equations were used to calculate cadmium adsorption onto barley ash. Then, as reported in, isotherm studies were performed.

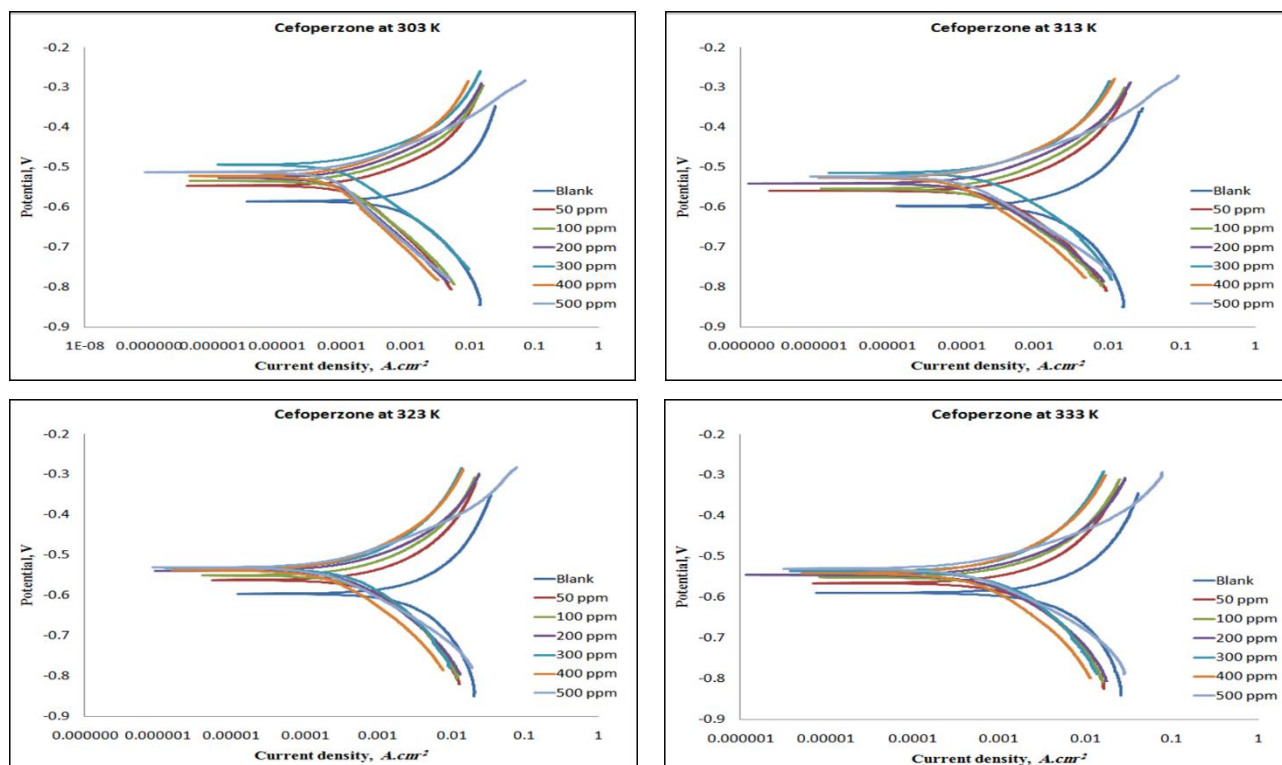


Figure 2: Polarization curves of corrosion inhibition by *Cefoperzone* at four temperatures.

Table 1: Corrosion data of *Cefoperzone* inhibitor in simulated fuel medium at four temperatures.

Conc. ppm	Temp. K	$-E_{corr}$ V	$i_{corr} \times 10^{-2}$ A.cm ⁻²	$\frac{-b_c}{+b_a}$ mV.dec ⁻¹		C_R mm/y	R_p Ω.cm ²	IE %
Blank	303	0.585	0.17187	250.54	163.41	20.162	24.98	---
	313	0.597	0.3611	317.3	227.91	42.361	15.94	---
	323	0.596	0.8995	541.56	351.36	105.52	10.28	---
	333	0.589	1.9523	967.69	512.68	229.02	7.45	---
50	303	0.546	0.0267	215.94	110.65	3.137	118.98	84.47
	313	0.559	0.0559	198.23	133.12	6.5532	61.86	84.52
	323	0.562	0.1646	277.89	178.67	19.309	28.68	81.70
	333	0.565	0.34136	346.07	239.42	40.046	18.00	82.51
100	303	0.534	0.01775	180.64	98.486	2.0824	155.91	89.67
	313	0.554	0.0298	164.53	114.88	3.4959	98.56	91.75
	323	0.550	0.0850	200.7	142.75	9.9749	42.61	90.55
	333	0.551	0.2002	263.45	183.33	23.485	23.44	89.75
200	303	0.526	0.0135	198.78	93.578	1.5825	204.64	92.15
	313	0.540	0.0212	148.7	101.65	2.4858	123.66	94.13
	323	0.539	0.0605	178.72	122.53	7.1001	52.17	93.27
	333	0.545	0.1410	210.71	149.6	16.546	26.94	92.78
300	303	0.494	0.0160	148.93	97.096	1.8724	159.51	93.25
	313	0.514	0.0392	163.22	134.58	4.6019	81.70	95.82
	323	0.533	0.0748	203.96	163.22	8.773	52.63	96.28
	333	0.536	0.1906	278.05	226.78	22.357	28.45	95.11
400	303	0.522	0.0116	221.41	101.46	1.3629	260.44	90.69
	313	0.527	0.0151	173.2	102.87	1.7662	185.58	89.14
	323	0.538	0.0335	171.6	123.19	3.9333	92.94	91.68
	333	0.541	0.0955	226.04	159.67	11.2	42.54	90.24
500	303	0.512	0.0103	203.52	73.627	1.21	227.93	94.01
	313	0.524	0.0137	125.99	76.85	1.6022	151.29	96.21
	323	0.531	0.0257	118.76	83.214	3.0154	82.66	97.14
	333	0.530	0.0673	133.21	93.695	7.8954	35.48	96.55

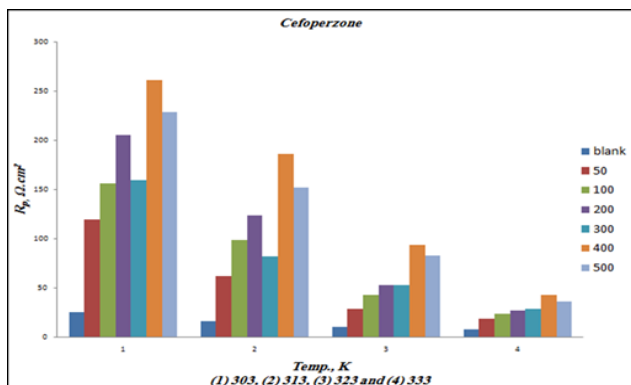


Figure 3: Polarization resistance behavior after inhibition by Cefoperazone.

Kinetic Properties and Mechanism

The rate of corrosion (C_R) in an experimental environment is directly proportional with values of corrosion current density (i_{corr}) according to the Arrhenius Equ.(7), as follows:

$$i_{corr} = A \cdot e^{-E_a/RT} \quad (7)$$

Where: A is a pre-exponential factor and E_a is activation energy which is estimated from the slope of plotting $\log i_{corr}$ versus $\frac{1}{T}$, while T and R are temperature in Kelvin and gas constant (see Figure 4). Activation energies in presence of Cefoperazone varied with concentration (see Table 2) which due to variation in active centers that have electron affinity to the positively charged metallic surface to be adsorbed on it such as nitrogen atoms ($-N-$) within rings, amine groups ($-NH-$), carbonyl groups ($>C=O$), carboxylic group, sulfur atoms ($-S-$) and phenol group that work by act a barrier between the surface of the metallic and corrosive species as illustrated in suggested mechanism in Figure 5.

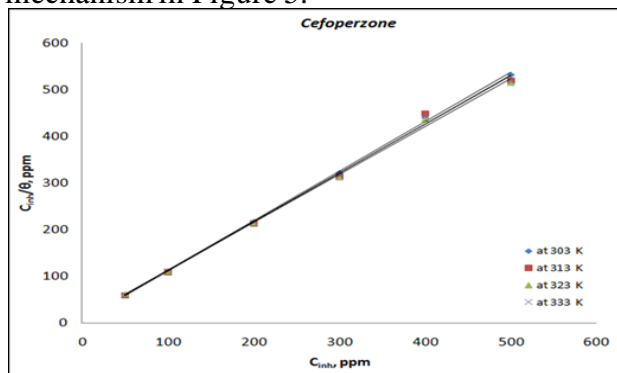


Figure 4: Arrhenius plots for inhibition.

Table 2: Activation energies for corrosion and inhibition.

Conc., ppm	E_a , kJ.mol ⁻¹
Blank	29.858
50	31.768
100	30.203
200	29.352
300	29.408
400	25.749
500	22.638

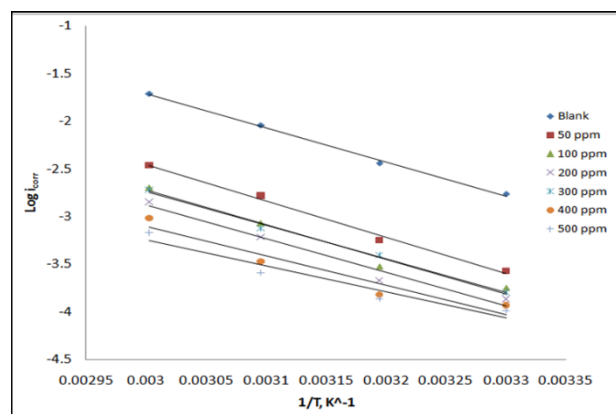


Figure 5: Langmuir adsorption isotherm plots.

Adsorption Isotherm

Adsorption is primarily influenced by a variety of aspects of the metallic surface and the types of hindered molecules with activity centers. Physical adsorption and chemical adsorption are the two interactions that lead to the attachment of the inhibitor with the surface of the metal during adsorption. The degree of surface covering (θ) for different inhibitor concentrations has been estimated using Equ. (8) to derive the adsorption isotherm.:

$$\theta = IE\% \div 100 \quad (8)$$

Langmuir adsorption isotherm is given by the Equ. (9):

$$\frac{C_{inh}}{\theta} = \frac{1}{K_{ads}} + C_{inh} \quad (9)$$

where C_{inh} represents the concentration of the inhibitor inside the bulk medium and K_{ads} represent the equilibrium constant of the adsorption-desorption process., the plotting of C_{inh}/θ versus C_{inh} at experimental temperatures gives straight lines (see Figure 6) that confirm the obeying to Langmuir adsorption isotherm, where the linear regression coefficient close to one with R^2 values in the range of $0.999 > R^2 >$

0.995 as listed in Table 3. The Langmuir isotherm is based on the hypothesis that each spot of the metal surface has one molecule adsorbed there (Drug). Consequently, one of the drug molecules replaces one of the adsorbed H_2O molecules. [23]. To determine the apparent free energy of adsorption (ΔG°_{ads}), the following relation was used [24].

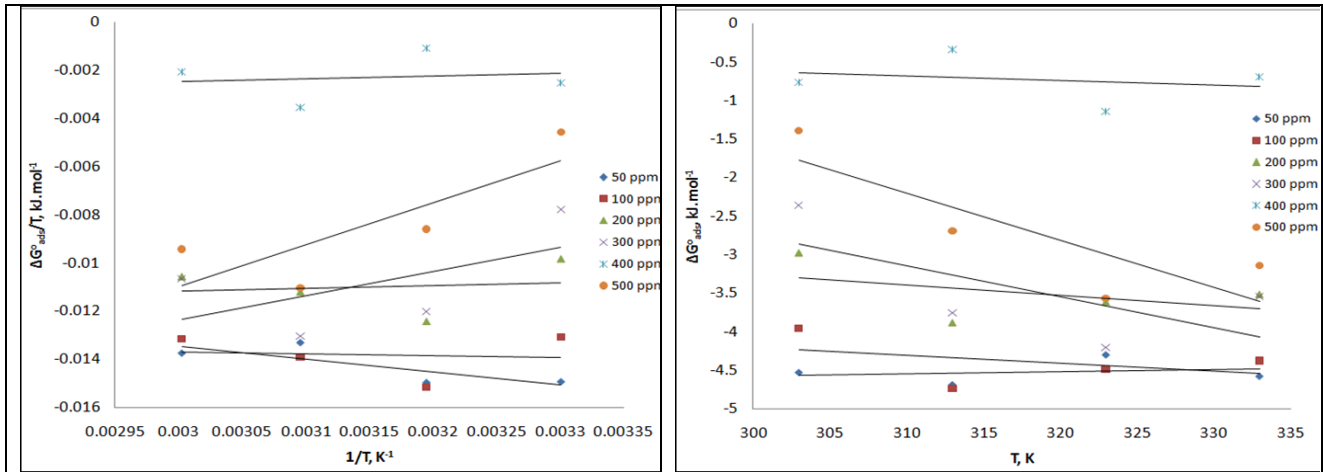


Figure 6: The relation between free energy and temperature for adsorption.

Table 3: R^2 values for adsorption.

Temp. (K)	R^2 value
303	0.999
313	0.995
323	0.997
333	0.997

$$\begin{aligned} \Delta G^{\circ}_{ads} &= -2.303RT \log 55.5 K_{ads}, \quad \text{where } K_{ads} \\ &= \frac{\theta}{C_{inh}(1-\theta)} \end{aligned} \quad (10)$$

The values of K_{ads} and ΔG°_{ads} are shown in Table 4.

The negative values of ΔG°_{ads} demonstrated the drug's spontaneous adsorption and the very minimal interaction between the surface of the metal and the inhibitor. Revealing the physical adsorption interaction between the drug molecules on the steel surface and the adsorbed drug molecules, the values of K_{ads} are comparatively low, which is supported by low negative values. (ΔG°_{ads}), where the (ΔG°_{ads}) values reach -20 kJ/mol imply physical adsorption and are compatible with electrostatic

interactions between the charged molecules and the charged metal surface.

The enthalpy of adsorption (ΔH°_{ads}) can be calculated from the Gibbs–Helmholtz equation [25]:

$$\frac{\Delta G^{\circ}_{ads}}{T} = \frac{\Delta H^{\circ}_{ads}}{T} + K_{ads} \quad (11)$$

Plotting $\frac{\Delta G^{\circ}_{ads}}{T}$ versus $\frac{1}{T}$ leads to get ΔH°_{ads} from slopes of straight lines as in Figure 6) and the data are showed in Table (5). The negative sign of ΔH°_{ads} was shown for 50 and 100 ppm indicating the exothermic process which suggest either physic- or chemisorption, while the positive sign was obtained for 200, 300, 400 and 500 ppm which indicating the endothermic process for adsorption that suggest a chemisorption of Cefoperzone. To calculate the entropy of adsorption ΔS°_{ads} , the following equation can be used shown in Figure 6 to calculate Equ. (12):

$$\left[\frac{\partial(\Delta G^{\circ}_{ads})}{\partial T} \right]_P = -\Delta S^{\circ}_{ads} \quad (12)$$

The value of ΔS_{ads}^o is positive that reflecting the increase randomness at the metal/solution interface as shown in Table 5.

Table 4: Parameters of adsorption isotherm for inhibition on by *Cefoperzone* at four temperatures.

Temp., K	Conc., ppm	K_{ads}	$-\Delta G_{ads}^o, kJ.mol^{-1}$
303	50	0.108783	4.53019
	100	0.086805	3.961553
	200	0.058694	2.975567
	300	0.046049	2.364243
	400	0.024353	0.759095
	500	0.031389	1.398589
313	50	0.109199	4.689635
	100	0.111212	4.737181
	200	0.080179	3.885615
	300	0.076411	3.760352
	400	0.02052	0.338463
	500	0.05077	2.6963
323	50	0.08929	4.298827
	100	0.09582	4.488418
	200	0.069294	3.617886
	300	0.086272	4.206498
	400	0.027548	1.140329
	500	0.06793	3.564483
333	50	0.094351	4.584596
	100	0.087561	4.377783
	200	0.064252	3.5207
	300	0.064833	3.545623
	400	0.023115	0.68977
	500	0.055971	3.138624

Table 5: The change in enthalpy and entropy for adsorption.

Conc., ppm	$\Delta H_{ads}^o, kJ.mol^{-1}.K^{-1}$	$\Delta S_{ads}^o, kJ.mol^{-1}$
50	-5.329	-0.0024
100	-0.818	0.0101
200	+1.202	0.0135
300	+10.136	0.0402
400	+1.142	0.0059
500	+17.450	0.0612

FESEM Examination

Figure 7 shows the morphology of the polished steel surface indicating a clean surface with some scratches during the grinding and polishing process, at two magnifications for all images. Figure 8 indicates the morphology of the corroded steel surface in a simulated fuel medium illustrating the damage at anodic and cathodic sites. While Figure 9 shows the morphology of inhibited surfaces by *Cefoperazone* with less risk through the adsorption of drug molecules on the surfaces that appear as flakes shaped structures to isolate the surface from a corrosive environment. The EDS analysis (see Figure 10) for polished surfaces shows the peak of iron (Fe) as a main element, as shown in Figure 10a, in steel composition, while after corrosion as illustrated in Figure 10b, it is known that the surface may form a passive layer to show the peaks for iron and oxygen O. Figure 10c highlights the EDS analysis for inhibited surface indicates the presence of carbon (C), oxygen (O) and sulfur (S) due to adsorption of drug molecules that contain these elements in their chemical formula.

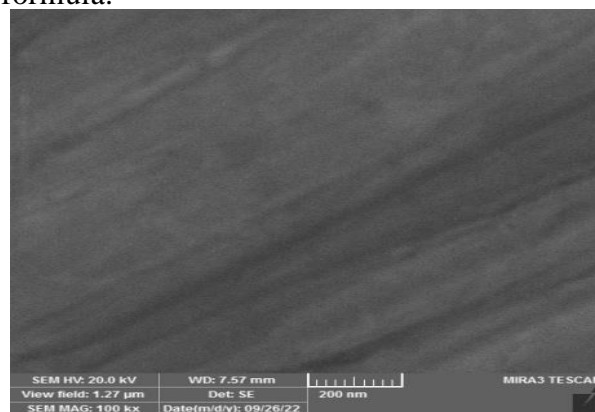
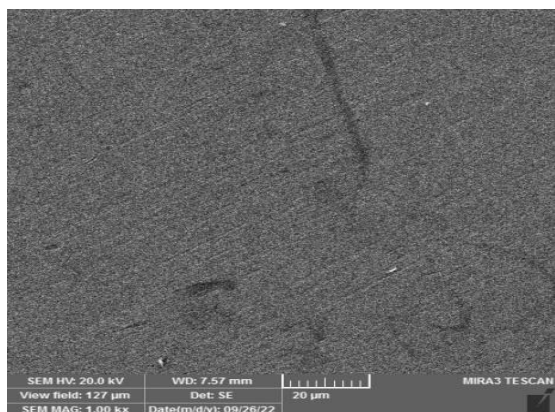


Figure 7: FESEM of corroded base specimen.

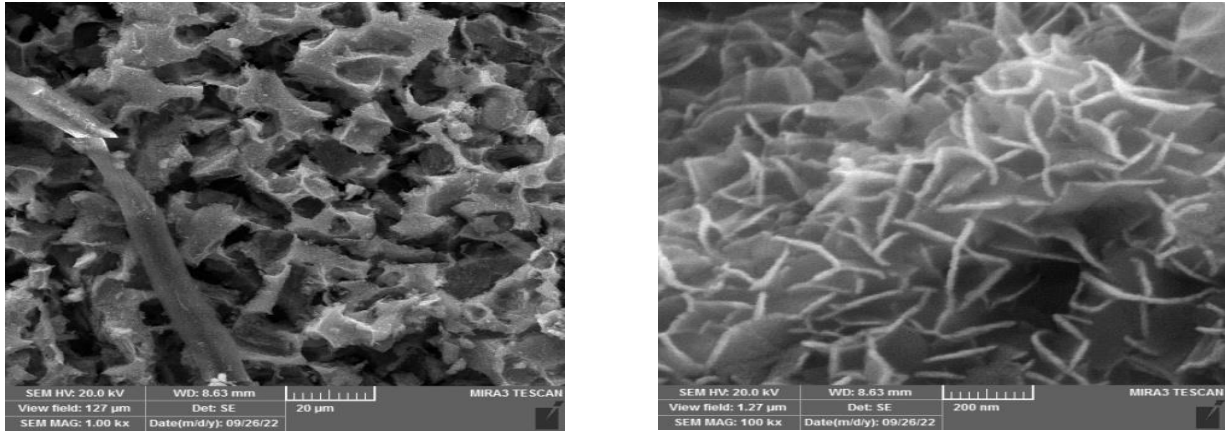


Figure 8: FESEM of corroded base specimen.

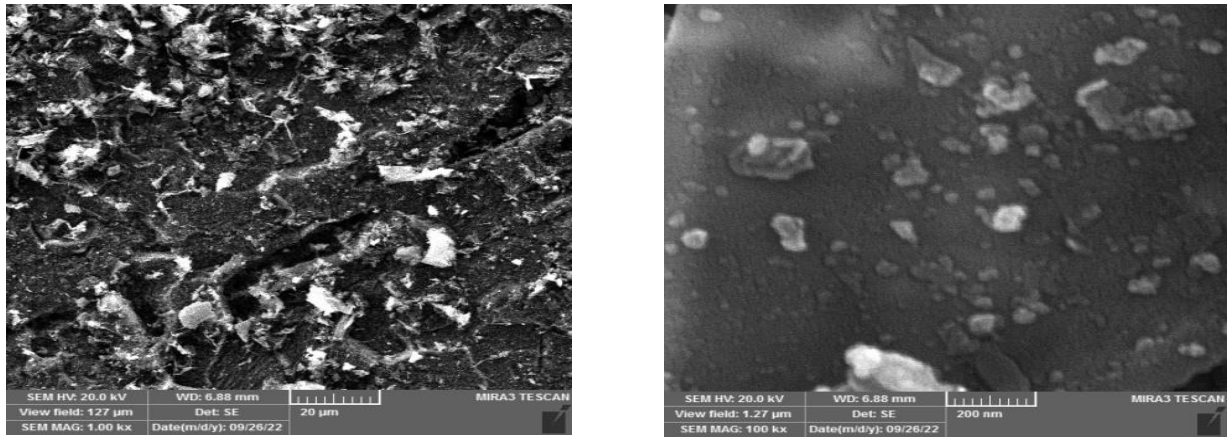


Figure 9: FESEM of inhibited specimen.

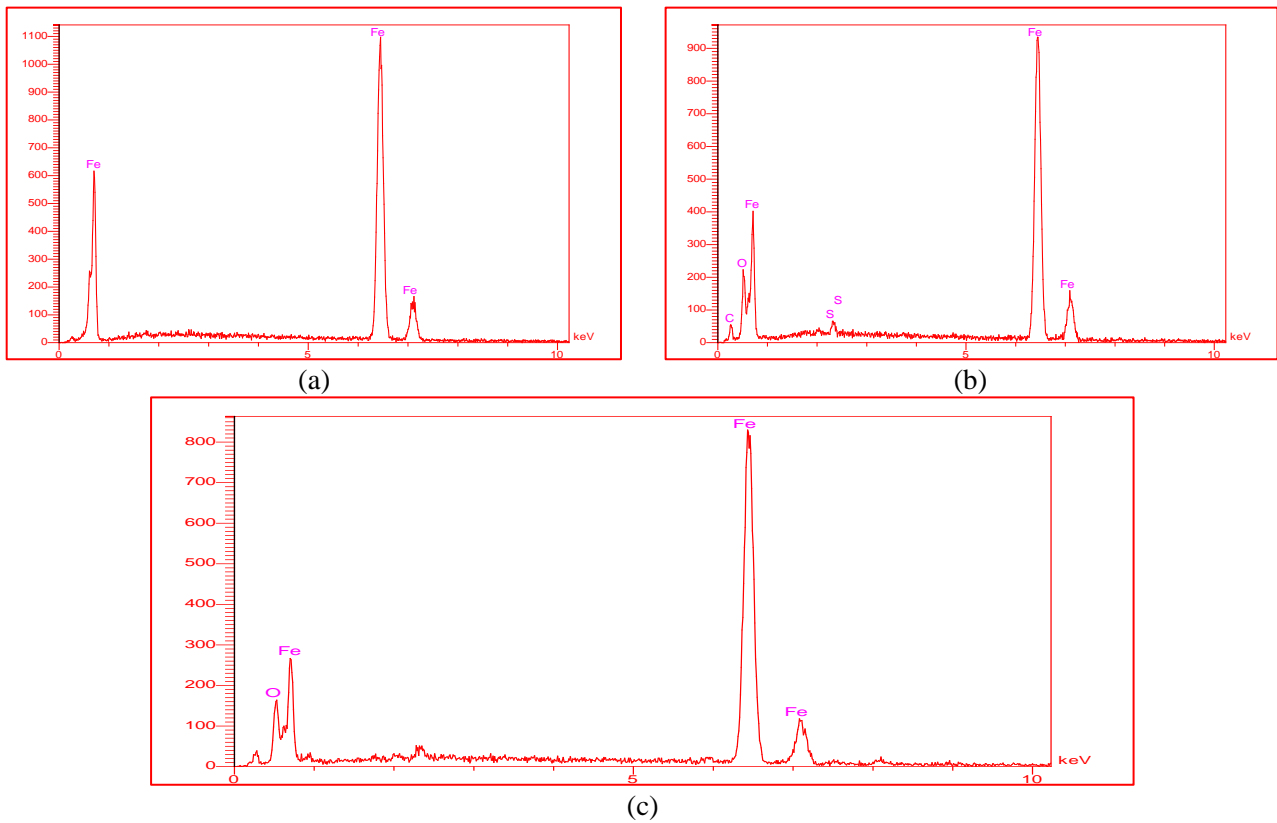


Figure 10: EDX analysis of polished, corroded and inhibited specimen.

AFM Examination

Figure 11 shows the topographical exam of the polished surface in two (2D) and three (3D) dimensions with the columns -shaped topography due to the grinding and polishing process followed by the presence of some valleys and peaks in the corroded surface due to pits as anodic sites (see Figure 12) with increase in values of the root-mean-square height (R_q), the arithmetic mean height (R_a), maximum height (R_z), and developed interfacial area ratio (R_{dr}) as listed in Table 6. The increasing in surface roughness (R_a) from 12.97nm to

307.1nm is due to corrosion damage. Figure 13 shows the topography for inhibited surfaces by the drug's molecules indicating clear adsorption of molecules on the surfaces with decreasing in the data of AFM analysis, where the maximum height (R_z) is reduced and the surface roughness (R_a) also reduced to 83.15 nm. Figure 14 shows the profile for surfaces that have been polished, rusted, and inhibited, with variation in mean depth as 10.56 nm for polished, 235.9 nm for corroded, and 99.71 nm for inhibited surfaces.

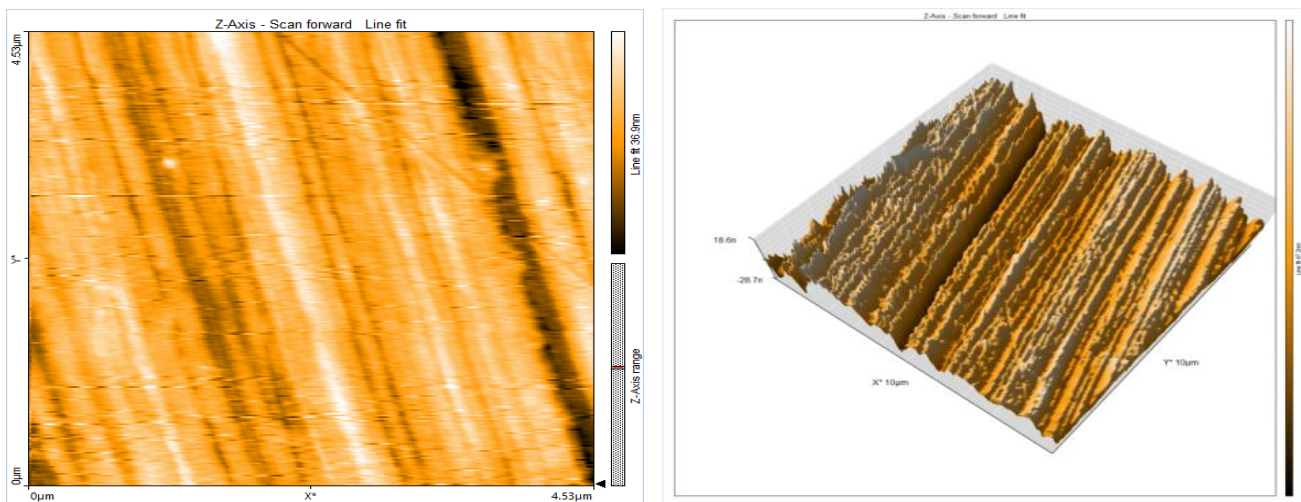


Figure 11: 2D and 3D images for polished steel surface.

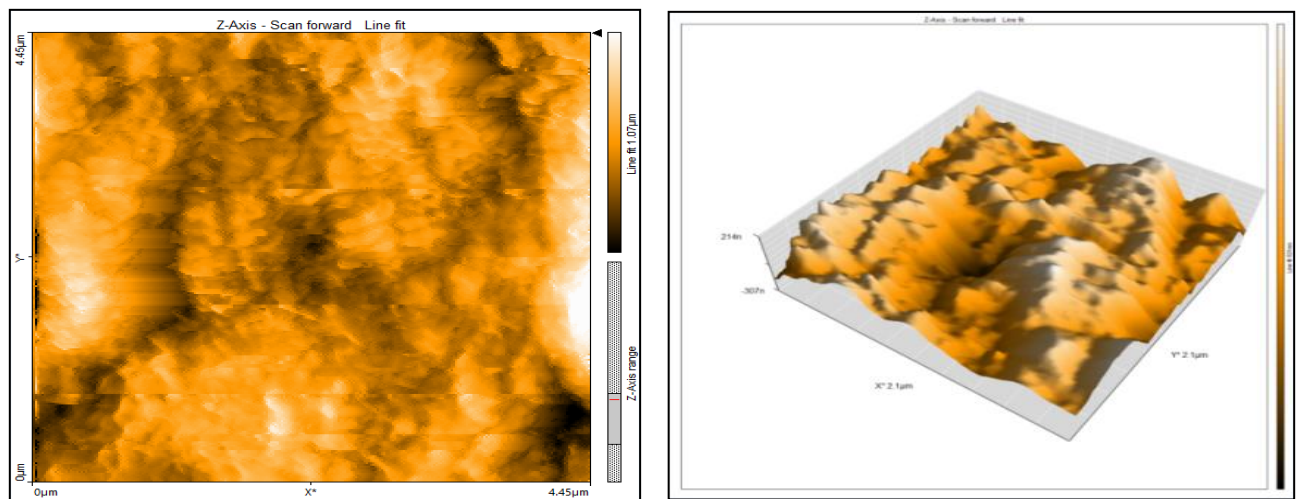


Figure 12: 2D and 3D images for corroded steel surface.

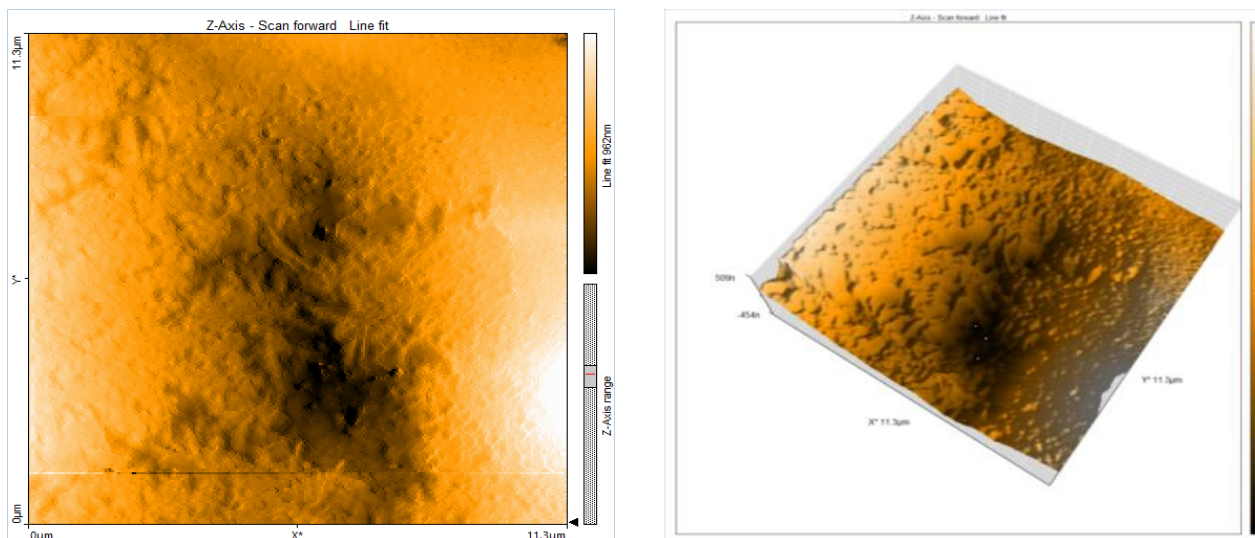


Figure 13: 2D and 3D images for inhibited steel surface.

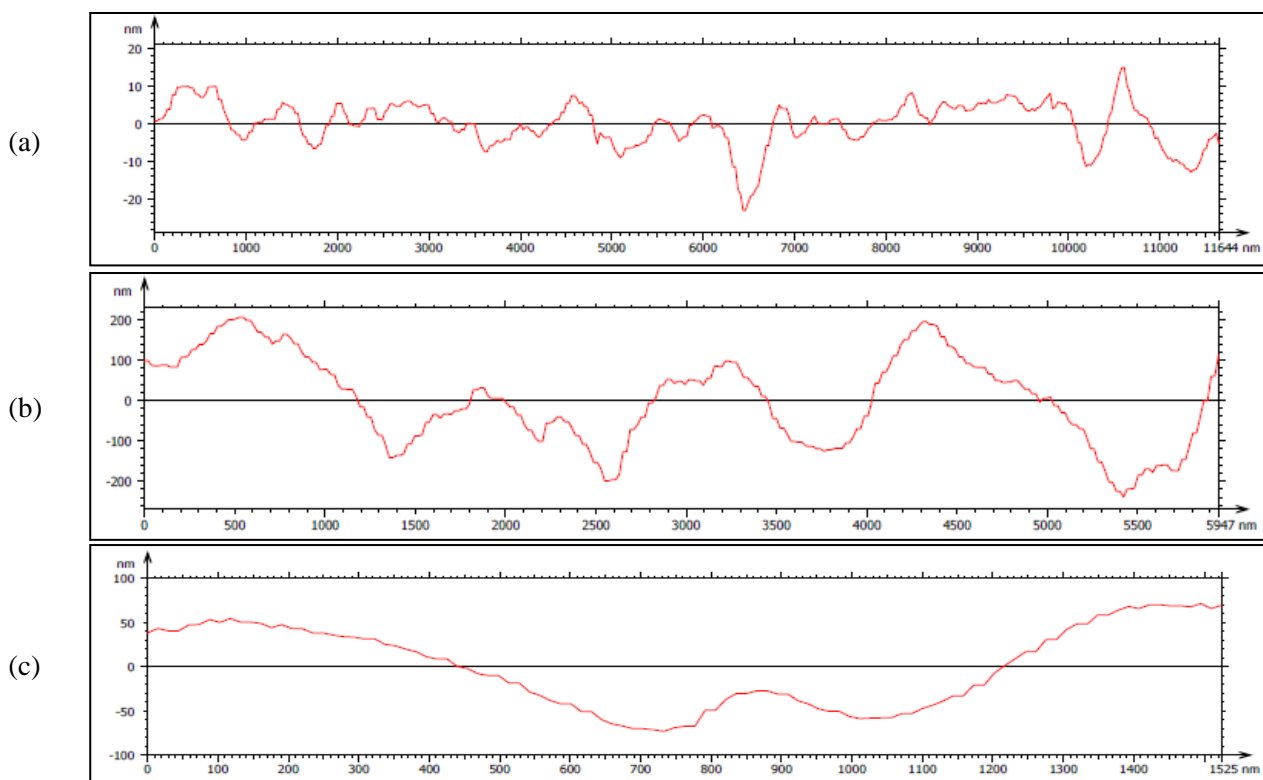


Figure 14: Profile of topography of: (a) polished, (b) corroded, and (c) inhibited.

Table 6: AFM data of samples.

Data	Polished surface	Corroded surface	Inhibited surface
Root-mean-square height (R_q)	15.51 μm	383.3 nm	101.8 nm
Maximum height (R_z)	98.47 μm	4357 nm	727.9 nm
Arithmetic mean height (R_a)	12.97 μm	307.1 nm	83.15 nm
Developed interfacial area ratio (R_{dr})	0.6077 %	76.55 %	13.79 %

CONCLUSIONS

On mild steel surfaces, the anti-corrosion potency of six concentrations of Cefoperazone derivatives (50, 100, 200, 300, 400, and 500

ppm) was evaluated in simulated oil well water (SOWW). 303–333 Kelvin can be measured via polarization and a potentiostat. The efficiency of the inhibitor has been verified

using a variety of methods, including a study of thermodynamics, theoretical calculations, and an analysis of the morphology of the metallic exterior. These researches led to the following findings, which are simplified into the following:

- The measurement of polarization reveals that Cefoperazone inhibitor achieved the greatest level of 97.14% inhibition efficiency, the concentration at 323 K (500 ppm).
- Based on the Tafel extrapolation curve inhibitor, the medicine Cefoperazone works as a mixed-type inhibitor.
- The physical contact of this chemical on the corroded metal causes the inhibitory efficiency of the Cefoperazone inhibitor to increase as the temperature rises from 303 K to 333 K. and a steel surface free of corrosion.
- The inhibitory mechanism's isotherm complies with model of Langmuir.
- The interaction between an inhibitor and a steel surface is suggested by the low free energy and equilibrium constant values.
- The adsorption of molecules falls under the area of physical adsorption.
- The SEM/EDS data supported the adsorption process, by employing AFM while applying Cefoperazone inhibitor to the steel surface to decrease the number of cracks and pits. The findings revealed that the average surface roughness increased as a result of the steel's protective coating.

ACKNOWLEDGMENTS

Grateful and appreciations are submitted to Mustansiriyah University Baghdad/Iraq, <https://www.uomustansiriyah.edu.iq> for its support to achieve this work.

Disclosure and Conflicts of Interest: The authors advertise that they have no conflicts of interest.

REFERENCES

- [1] Chaouiki, H. Lgaz, I.-M. Chung, I. H. Ali, S. L. Gaonkar, K. S. Bhat, R. Salghi, H. Oudda, and M. I. Khan, "Understanding corrosion inhibition of

mild steel in acid medium by new benzonitriles: Insights from experimental and computational studies", *Journal of Molecular Liquids*, Vol. 266, pp. 603-616, 2018.

- [2] Rebak, Raul B., and Teresa E. Perez. "Effect of carbon dioxide and hydrogen sulfide on the localized corrosion of carbon steels and corrosion resistant alloys", *NACE International, corrosion conference & expo*, 2017.
- [3] V. N. Ayukayeva, G. I. Boiko, N. P. Lyubchenko, R. G. Sarmurzina, R. F. Mukhamedova, U. S. Karabalin, and S. A. Dergunov, "Polyoxyethylene sorbitan trioleate surfactant as an effective corrosion inhibitor for carbon steel protection", *Colloids and Surfaces A: Physicochemical and Engineering Aspects*, Vol. 579, pp. 123636, 2019.
- [4] H. Ouici, M. Tourabi, O. Benali, C. Selles, C. Jama, A. Zarrouk, and F. Bentiss, "Adsorption and corrosion inhibition properties of 5-amino 1, 3, 4-M. E. Belghiti, Y. Karzazi, A. Dafali, I. B. Obot, E. E. Ebenso, K. M. Emran, I. Bahadur, B. Hammouti, F. Bentiss, *J. Mol. Liq.* 2016, 216, 874–886..
- [5] M. Farsak, A. Ongun Yüce, and G. Kardaş, "Anticorrosion effect of 4- amino-5-(4-pyridyl)-4H-1, 2, 4-triazole-3-thiol for mild Steel in HCl Solution", *ChemistrySelect*, Vol. 2, No. 13, pp. 3676-3682, 2017.
- [6] M. Prajila, and A. Joseph, "Inhibition of mild steel corrosion in hydrochloric using three different 1,2,4-triazole Schiff's bases: A comparative study of electrochemical, theoretical and spectroscopic results", *Journal of Molecular Liquids*, Vol. 241, pp. 1-8, 2017.
- [7] P. R. Ammal, M. Prajila, and A. Joseph, "Effect of substitution and temperature on the corrosion inhibition properties of benzimidazole bearing 1, 3, 4-oxadiazoles for mild steel in sulphuric acid: Physicochemical and theoretical studies", *Journal of Environmental Chemical Engineering*, Vol. 6, No. 1, pp. 1072-1085, 2018.
- [8] A. Maharramov, Y. Mamedova, M. Bayramov, and I. Mamedov, "Chalcone derivatives as corrosion inhibitors for mild steel in brine-kerosene solution", *Russian Journal of Physical Chemistry A*, Vol. 92, No. 11, pp. 2154-2158, 2018.
- [9] Y. El Bakri, L. Guo, E. H. Anouar, and E. M. Essassi, "Electrochemical, DFT and MD simulation of newly synthesized triazolotriazepine derivatives as corrosion inhibitors for carbon steel in 1 M HCl", *Journal of Molecular Liquids*, Vol. 274, pp. 759-769, 2019.

- [10] Q. H. Zhang, B. S. Hou, N. Xu, H. F. Liu, and G. A. Zhang, "Two novel thiadiazole derivatives as highly efficient inhibitors for the corrosion of mild steel in the CO₂-saturated oilfield produced water", *Journal of the Taiwan Institute of Chemical Engineers*, Vol. 96, pp. 588-598, 2019.
- [11] E. Taflan, H. Bayrak, M. Er, Ş. A. Karaoğlu, and A. Bozdeveci, "Novel imidazo [2, 1-b][1, 3, 4] thiadiazole (ITD) hybrid compounds: Design, synthesis, efficient antibacterial activity and antioxidant effects", *Bioorganic chemistry*, pp. 102998, 2019.
- [12] S. K. Ahmed, W. B. Ali, and A. A. Khadom, "Synthesis and investigations of heterocyclic compounds as corrosion inhibitors for mild steel in hydrochloric acid", *International Journal of Industrial Chemistry*, Vol. 10, No. 2, pp. 159- 173, 2019.
- [13] I. Merimi, Y. El Ouali, R. Benkaddour, H. Lgaz, M. Messali, F. Jeffali, and B. Hammouti, "Improving corrosion inhibition potentials using two triazole derivatives for mild steel in acidic medium: Experimental and theoretical studies", *Materials Today: Proceedings*, Vol. 13, pp. 920-930, 2019.
- [14] PRABHA, A. Suriya, et al. Inhibition of corrosion of mild steel in simulated oil well water by an aqueous extract of *Andrographis paniculata*. 2020.
- [15] ODUNLAMI, Olayemi Abosede, et al. Chemical Adsorption Data's, Temperature Effect and Structural Properties of Artemether-Lumefantrine Corrosion Inhibition Properties on Structural Steel in 0.62 M NaCl. In: *Key Engineering Materials*. Trans Tech Publications Ltd, 2021. p. 143-155.
- [16] Nithya K & Devi Meenakshi, *Int J Nano Corr Sci Eng*, 3 (2016) 44.
- [17] Noor Najm, Ali H. Ataiwi, Rana A. Anae, Annealing and coating influence on the mechanical properties, microstructure, and corrosion properties of biodegradable Mg alloy (AZ91), *Journal of Bio- and Tribo-Corrosion*, 8 (2022) 64.
- [18] Rana Afif Anae, Abdullah A. Abdulkarim, Mathew T. Mathew, Hiyam Mezher Jedy, The Effect of Nb₂O₅-Ni Coatings on the Microstructural and Corrosion Behavior on Carbon Steel for Marine Application. *Journal of Bio- and Tribo-Corrosion* 7:1 (2021).
- [19] Hiba A. Abdullah, Raad Suhail Ahmed Adnan, Rana A. Anae, Deposition of CaO to protect carbon steel by electrophoretic method, *Materials Today: Proceedings*, (2021), in press.
- [20] R.A. Anae, Behavior of Ti/HA in Saliva at Different Temperatures as Restorative Materials, *Journal of Bio- and Tribocorrosion*, 2 (5), 2016, DOI 10.1007/s40735-016-0036-1
- [21] Noor Najm, Ali H. Ataiwi, Rana A. Anae, Effect of indium coating on corrosion behavior of AZ31 Mg alloy by DC sputtering, *Materials Today: Proceedings*, (2021), in press.
- [22] Rana Anae, Thermodynamic and kinetic study for corrosion of Al-Si-Cu/Y₂O₃ composites, *Asian Journal of Chemistry*, 2014, 26(14), pp. 4469–4474
- [23] T.A. Alkarim, K.F. Al-Azawi and R.A. Anae, Anticorrosive properties of Spiramycin for aluminum in acidic medium. *Int. J. Corros. Scale Inhib*, 10(3), 1168–1188 (2021).
- [24] Thekra Abd Alkarim, Khalida F. Al Azawi and Rana Afif Anae, Green approach to corrosion inhibition of aluminum in acidic solutions by the expired drug and biological activity", *Biochem. Cell. Arch.*, 21(2), 3557-3569, 2021.
- [25] Abdullah, R.A. Anae and A.A. Khadom, Expired Methprim drug as a corrosion inhibitor for aluminum in 1 M HCl solution: Experimental and theoretical studies, *Int. J. Corros. Scale Inhib.*, 2022, 11(3), 1355–1373.

How to Cite

A. M. . Kadhim, R. A. . Anae, M. J. . M. Hassan, and M. A. I. . Al-lami, "Study the Corrosion Inhibition on the Iraqi Fuel Tanks using Cefoperazone Drug", *Al-Mustansiriyah Journal of Science*, vol. 34, no. 3, pp. 31–42, Sep. 2023.

